



## **DYNAMIC PROPERTIES OF SINTERED MOLYBDENUM STEELS**

by

S. St-Laurent and F. Chagnon

Quebec Metal Powders Limited

Paper presented at the PM World Congress  
June 16 – June 21, Orlando, U.S.A.

# **DYNAMIC PROPERTIES OF SINTERED MOLYBDENUM STEELS**

Sylvain St-Laurent and Francois Chagnon

Quebec Metal Powders Limited  
Tracy, Québec

## **ABSTRACT**

A large number of P/M applications require sintered components capable of withstanding high operational static and dynamic stresses. Raising sintered density is one of the key parameters to enhance dynamic properties together with appropriate microstructure. Amongst the low alloyed steel powders available on the market, low alloy Mo powders present interesting attributes because this alloying element only slightly affects powder compressibility and is very efficient to increase hardenability and hence mechanical properties. Furthermore, the addition of key elemental additives such as Ni and Cu admixed to the base steel powders or diffusion bonded to the steel particles during the annealing treatment also contributes to improve the mechanical properties through modification of the microstructure.

This paper reports the results of a study to characterize the tensile and dynamic properties of low alloy steel powders containing various levels of pre-alloyed molybdenum. The effect of either admixing or diffusion bonding Ni and Cu to these Mo steels is also discussed particularly with respect to axial fatigue properties and strength. Comparison with results obtained with other types of fatigue specimens and/or testing methods is also presented.

## **I. INTRODUCTION**

The number of highly performance applications requiring sintered P/M components capable of withstanding severe operational stresses is continuously increasing. To attain the mechanical properties required for these demanding applications, the chemistry, microstructure, cleanliness and density must be optimized. In particular, pores that are inevitably present in sintered components play a key role in the fatigue crack initiation and propagation [1,2]. It is well known that decreasing the proportion of pores by increasing the density is highly beneficial for the fatigue strength of parts [3,4,5].

In recent years, numerous developments and improvements related to the compaction technology such as warm compaction and the performance and quality of steel powders have considerably increased the density that can be reached as well as the attainable level of strength and fatigue resistance. In particular, a wide range of steel powder grades with different types and levels of alloying elements added either to the melt prior to atomization (pre-alloyed steel powder) or during the annealing treatment (diffusion-bonded powder) are available in the market depending on the hardenability requirement. However, raising the concentration of alloying elements in the steel powders usually leads to a deterioration of the powder compressibility [6]. In that sense, molybdenum is a very interesting pre-alloying element since it is very efficient in increasing strength with only a minor effect on powder compressibility as shown in Figure 1. This is why molybdenum low alloy steel powders are widely used to achieve high green density after compaction and high strength after sintering. Also, elements such as nickel and copper can be either admixed or diffusion-bonded to further increase the hardenability and strength of P/M components while maintaining compressibility. Pre-alloyed Mo steel powders containing 0.85% Mo admixed with Ni, Cu and graphite allows the formation of complex microstructures that are beneficial to the static and dynamic properties [7]. Such formulations are widely used for highly stressed applications. An extensive study of the tensile and dynamic properties of ATOMET 4401-Ni-Cu-C mixes carried out by Chagnon and Trudel [4] showed that the fatigue limit is optimized at 4% Ni, 1% Cu and 0.6% graphite within the limit of that study. However, according to the model developed in that study, a slightly higher fatigue limit should be obtained at 1.5% Cu. Figure 2 shows the rotating bending fatigue (RBF) limit of different FLN-0205 and FLN-4405 materials.

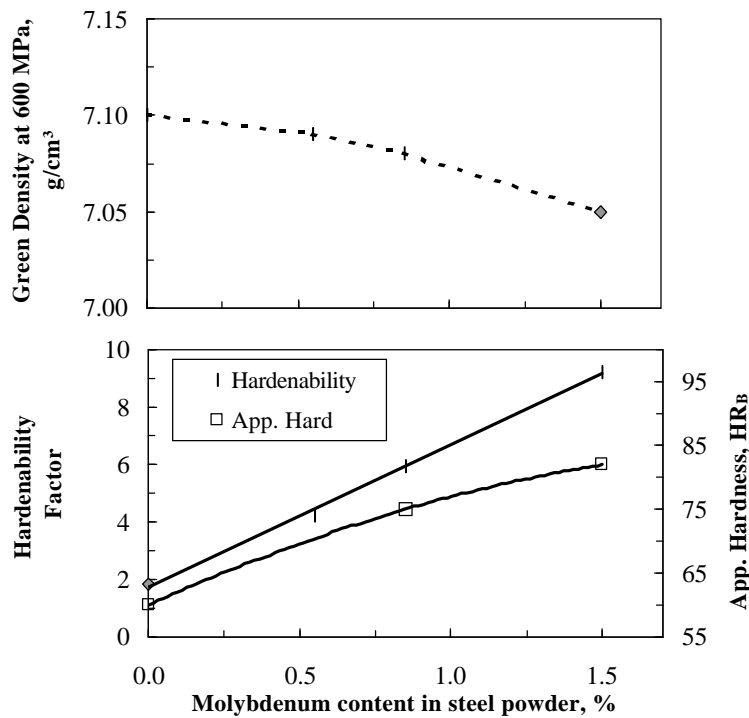


**Figure 1.** Variation of compressibility, calculated hardenability factor and apparent hardness as a function of the molybdenum content in steel powders (Mix formulation Steel + 0.8% C).

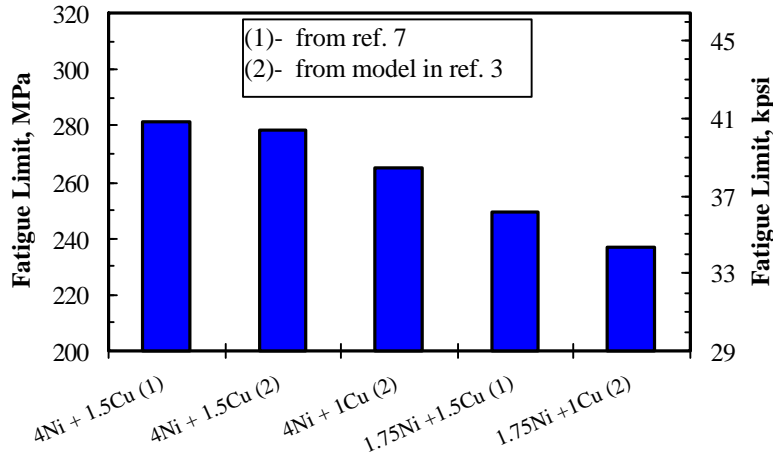


**Figure 2.** RBF fatigue limits obtained in different studies for a 0.85% pre-alloyed Mo steel powder at 7.0 g/cm<sup>3</sup>.

The object of the present paper is first to evaluate the influence of the level of Mo in steel powders from 0.5 to 1.5% on the tensile and dynamic properties of mixes containing 4% Ni, 1.5% Cu and 0.6% graphite at 7.0 g/cm. Particular attention is paid to the fatigue properties determined by axial fatigue testing. In particular, the S-N curves and the fatigue limit at 10<sup>7</sup> cycles are determined for five different mixes. A second objective of this study is to establish if the use of copper powders of different size could have an effect on the tensile and fatigue properties of such mixes. Indeed, a previous study showed that copper affects the size of porosity, when melting and penetrating into steel particles [8]. It was shown in different studies that the pores morphology and size affects the fatigue performance of sintered components [1]. Smaller pore size in association with rounded pores improved the fatigue performance at a given density. A regular and a binder-treated mix manufactured with a pre-alloyed 0.5% Mo steel powder and containing respectively a regular and a finer copper powder were evaluated and compared to a diffusion-bonded powder containing 0.5% pre-alloyed Mo with 4%Ni and 1.5% Cu partially diffused to steel particles.

## II. EXPERIMENTAL PROCEDURE

### Description of powder mixes

Water atomized pre-alloyed Mo steel powders containing either 0.5% Mo (ATOMET 4001), 0.85% Mo (ATOMET 4401) or 1.5% Mo (ATOMET 4901) were selected for this study together with a diffusion-bonded powder, ATOMET DB48 containing 0.5% Mo, 4%Ni and 1.5%Cu. All these powders contain about 0.15% Mn and 0.08% oxygen. The three pre-alloyed Mo steel powders were admixed with 4% nickel, 1.5% copper, 0.60% natural graphite and 0.75% wax, while the diffusion-bonded powder was admixed with 0.60% natural graphite and 0.75% wax. A commercial grade of Cu having with an average diameter D<sub>50</sub> of about 40µm was used in all these powder mixes. In addition to these powder mixes, a binder-treated mix made with the 0.5% Mo steel powder was prepared by using the QMP patented binder technology [9]. A fine commercial Cu grade having a D<sub>50</sub> of ~15 to 20 µm was used in this mix. The chemical composition and characteristics of the pre-alloyed and diffusion-bonded powders evaluated in this study as well as

the mixing technology are given in Table I. All the mixes had similar flow rate and apparent density except for the binder-treated mix that showed an improvement in flow rate of about 3.5 to 5.5 s/50 g as compared to the other mixes. A carbon content of 0.53% was achieved for all the materials after sintering.

**Table I.** Characteristics of the steel powders and pre-mixes evaluated in this study.

Mix name/ Steel powder	Type of mix	Pre-alloyed elements, wt%		Diffusion elements, wt%		Admixed elements, wt%			Flow, s/50g	A.D., g/cm <sup>3</sup>
		<i>Mo</i>	<i>Mn</i>	<i>Ni</i>	<i>Cu</i>	<i>Ni</i>	<i>Cu</i>	<i>Graphite</i>		
R-0.5Mo (ATOMET 4001)	Regular	0.5	0.15	-	-	4.0	1.5 (reg)	0.6	37.0	3.02
BT-0.5Mo (ATOMET 4001)	Binder- treated	0.5	0.15	-	-	4.0	1.5 (fine)	0.6	31.6	3.09
DB-0.5Mo (ATOMET DB48)	DB/ Regular	0.5	0.15	3.9	1.5	-	-	0.6	35.0	3.05
R-0.85Mo (ATOMET 4401)	Regular	0.85	0.15	-	-	4.0	1.5 (reg)	0.6	36.3	3.00
R-1.5Mo (ATOMET 4901)	Regular	1.5	0.15	-	-	4.0	1.5 (reg)	0.6	35.1	3.08

### **Description of flexural, tensile, impact and fatigue testing.**

Standard transverse rupture test specimens, flat tensile test specimens (dog bones) and blank specimens were pressed to a density of 7.0 g/cm<sup>3</sup> for each material. All green specimens were sintered for 25 min at 1120°C (2050°F) in a nitrogen base atmosphere containing 10% hydrogen in a commercial mesh-belt furnace. The cooling rate in the range of 650 - 400°C was about 0.65°C/sec. Half of the transverse rupture bars and all the tensile specimens were tempered 1 hre at 205°C (400°F) in air. Un-notched impact test specimens were machined out of the blank specimens. A tempering was done on the un-notched impact specimens under the same conditions as those used for the transverse rupture bar and tensile specimens.

The transverse sintered strength, dimensional change and apparent hardness were determined on transverse rupture bars in the as-sintered and as-tempered conditions. Tensile properties were determined on dog bones as per MPIF standard 10. The impact strength was determined according to MPIF standard 40. Three transverse rupture bars and four tensile and impact specimens were evaluated for each material and condition.

Standard ISO flat axial fatigue specimens were used to evaluate the fatigue properties of all these materials. Figure 3 shows the geometry and dimension of the flat specimens used in that study. The fatigue specimens were pressed to 7.0 g/cm<sup>3</sup>, sintered 25 min at 1120°C in a nitrogen base atmosphere and tempered one hour at 205°C in air. Specimens were smoothly polished. Axial fatigue testing was done in a fully reversed tension-compression loading mode (R= -1) with a sine waveform. A sample that survived more than 10<sup>7</sup> cycles was considered a runout. The staircase method was used to execute the test and determine the mean fatigue limit where 50% of the

specimens are expected to survive. The fatigue limit where 90% of specimens are expected to survive was also determined with this method.

The microstructure of TRS bars was evaluated after etching with Nital 2% by optical microscopy. The volume fraction, size and morphology of pores were determined by optical microscopy with a computer-aid Clemex image analysis system. The evaluation of porosity was performed at 200X on 300 to 360 fields, giving a total analyzed surface area of between 50 and 60 mm<sup>2</sup>. Fractographic analysis of fatigue specimens was done with a JEOL scanning electron microscope (SEM).

### III. RESULTS AND DISCUSSION

#### Compressibility

The compacting pressure at 7.0 g/cm<sup>3</sup> varied from 500 to 520 MPa for all the materials. Increasing the Mo content in steel powder from 0.5 to 1.5% led to only a slight increase in compacting pressure from 500 to 528 MPa. This confirms that molybdenum only slightly decreases compressibility as already reported and shown in Figure 1.

#### Sintered and tensile properties

The results of the transverse rupture and tensile tests carried out on tempered specimens are summarized in Table II. Figure 4 shows the effect of Mo content on the transverse rupture strength, apparent hardness of as-sintered and tempered specimens. Both the rupture strength and the apparent hardness in the as-sintered and tempered conditions first increased between 0.5 and 0.85% Mo and then leveled off above 0.85% Mo. As expected, the tempering led to a reduction in apparent hardness and an increase in TRS for all the materials. The dimensional change (DC)

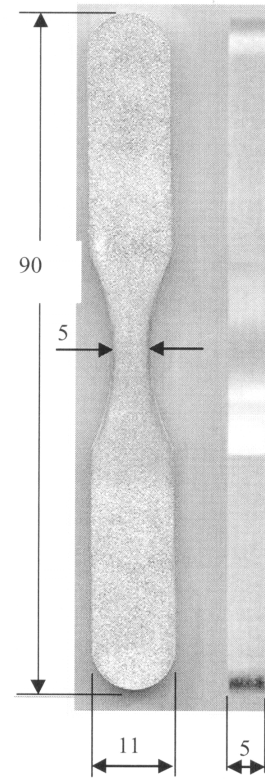


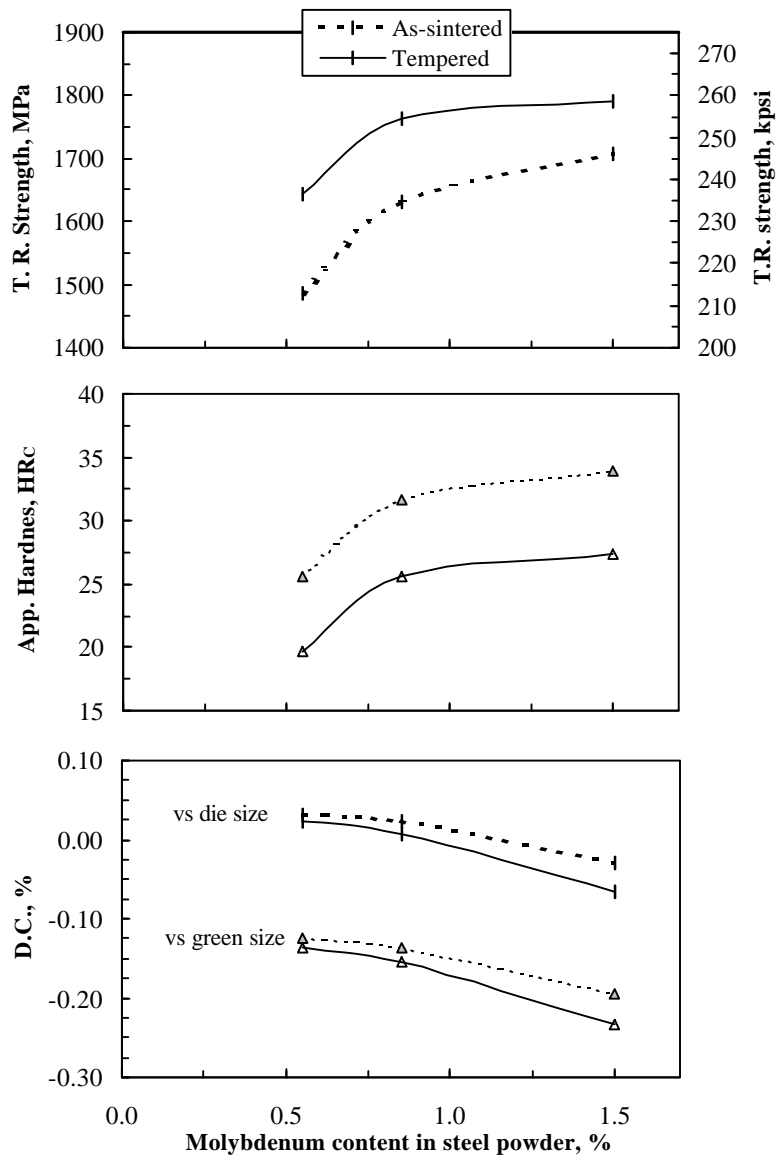
**Figure 3.** Test specimens used for the axial fatigue testing. Dimensions in mm.

**Table II.** Transverse and tensile properties of pre-alloyed Mo steel powders containing 4% Ni, 1.5% Cu and 0.6% graphite at 7.0 g/cm<sup>3</sup>.

Mix ID	TRS, MPa	App. Hard, HRC	DC vs die size, %	DC vs green size, %	UTS, MPa	YS, MPa	Elongation, %
R-0.5Mo	1644	20	0.02	-0.14	854	545	1.7
R-0.85Mo	1762	26	0.01	-0.15	924	580	1.2
R-1.5Mo	1791	27	-0.07	-0.23	937	587	1.0
R-0.5Mo	1644	20	0.02	-0.14	854	545	1.7
BT-0.5Mo	1688	21	-0.06	-0.22	845	569	1.6
DB-0.5Mo	1781	22	0.01	-0.17	848	544	1.2

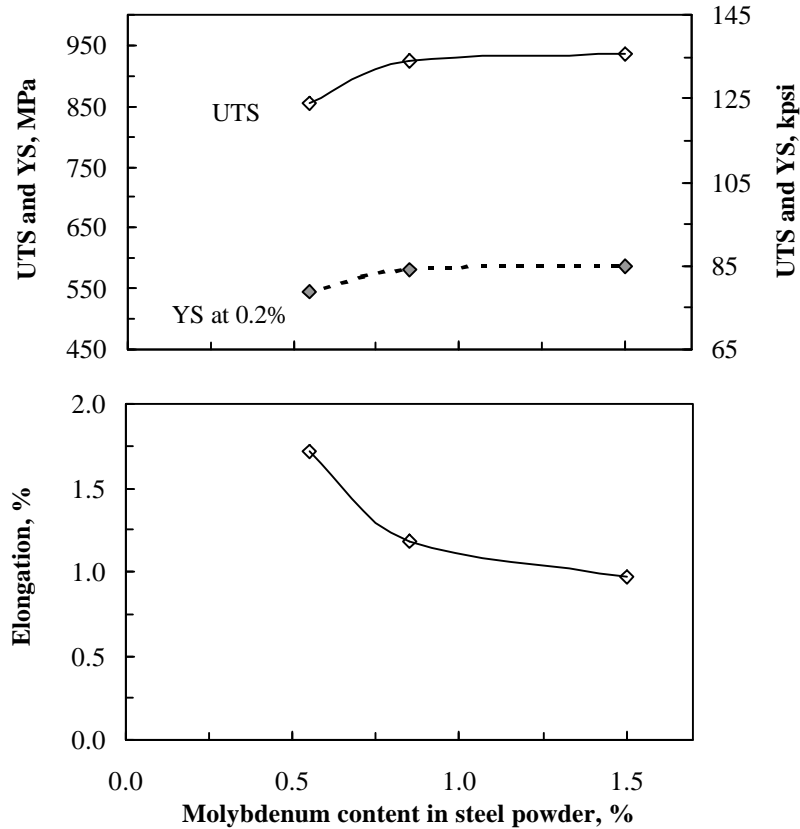
decreased with an increase in Mo content, the variation between 0.5 and 1.5% Mo being -0.06% in the as-sintered state and -0.09% after tempering. The DC was slightly more negative after tempering, the effect being more pronounced as the Mo content increased. As already shown in another study, this likely indicates that the proportion of martensite increased with the level of Mo [10].

Figure 5 shows the influence of Mo content on tensile properties. The trend was identical to that observed with the TRS : UTS and YS first increased between 0.5 and 0.85% and leveled off above 0.85%. The elongation followed the opposite trend and decreased from 1.7 to 1.0% by increasing the Mo content from 0.5% to 1.5%. The decrease in elongation was more pronounced between 0.5 and 0.85%.



**Figure 4.** Influence of the molybdenum content on the sintered strength, apparent hardness and dimensional change for specimens pressed to 7.0 g/cm<sup>3</sup> (4% Ni, 1.5% Cu, 0.6% graphite).

The sintered and tensile properties of the regular and binder-treated materials made with a 0.5% Mo steel powder and a diffusion-bonded material were quite similar. A slightly higher transverse rupture strength was obtained with the diffusion-bonded material. However, there was no significant difference in tensile and yield strength between these materials. The elongation of the diffusion-bonded powder mixes was also slightly lower. Finally, the DC of the binder-treated mix made with a fine grade of Cu was about 0.08% more negative than that obtained with a coarser grade. The use of a finer Cu grade yields to more important shrinkage during sintering. The DC of the diffusion-bonded material was similar to that of the regular grade.



**Figure 5.** Influence of molybdenum content on the UTS, YS at 0.2% offset and elongation for specimens pressed to 7.0 g/cm<sup>3</sup> from pre-alloyed powders admixed with 4% Ni, 1.5% Cu and 0.6% graphite.

### Microstructure and Porosity

Figure 6 shows the typical microstructure for the 0.5, 0.85 and 1.5% Mo materials admixed with 4% Ni, 1.5% Cu and 0.6% graphite. The microstructure was typical for that type of formulation, i.e. a heterogeneous microstructure constituted of areas of divorced pearlite, fine pearlite/bainite, martensite and Ni-rich retained austenite. The microstructure within steel particles where nickel did not diffuse changed gradually from divorced pearlite/pearlite/bainite to bainite/martensite as the amount of Mo increased. The higher proportion of martensite formed during sintering when Mo content increases is also illustrated by the change in dimensional change that occurred during tempering. Indeed, it was shown on a previous study on sinter-hardening steel powders that the variation in dimensional change during tempering was related to the proportion of martensite and

the level of carbon in the specimens [10]. The shrinkage obtained during tempering is due to the transformation of martensite from a tetragonal body-centered structure to a hexagonal structure [11].

It is well known that the admixed copper particles melt during sintering at about 1080°C and penetrates and diffuses into steel particles, leaving pores behind. The use of copper of different size should therefore affect the size of the residual pores. Figure 7 shows the cumulative pore count frequency as a function of the pore length (as determined by the maximum size of pores) in sintered specimens along with micrographs showing the porosity distribution. All the specimens made with materials admixed with a regular grade of copper show similar pore frequency distribution. The longest pores analyzed in these specimens were in the range of 190 to 200  $\mu\text{m}$ . However, in the binder-treated and diffusion-bonded materials, the number of pores per unit area above 50  $\mu\text{m}$  was significantly lower. In fact, the slope of the frequency distribution shown in Figure 7 was significantly much steeper for these materials than for the regular mix. As a result, the longest pores observed in sintered specimens were respectively about 140 and 155  $\mu\text{m}$  for the binder-treated and the diffusion-bonded materials. These analyses clearly show that the grade of copper used has a strong influence on the pore size distribution.

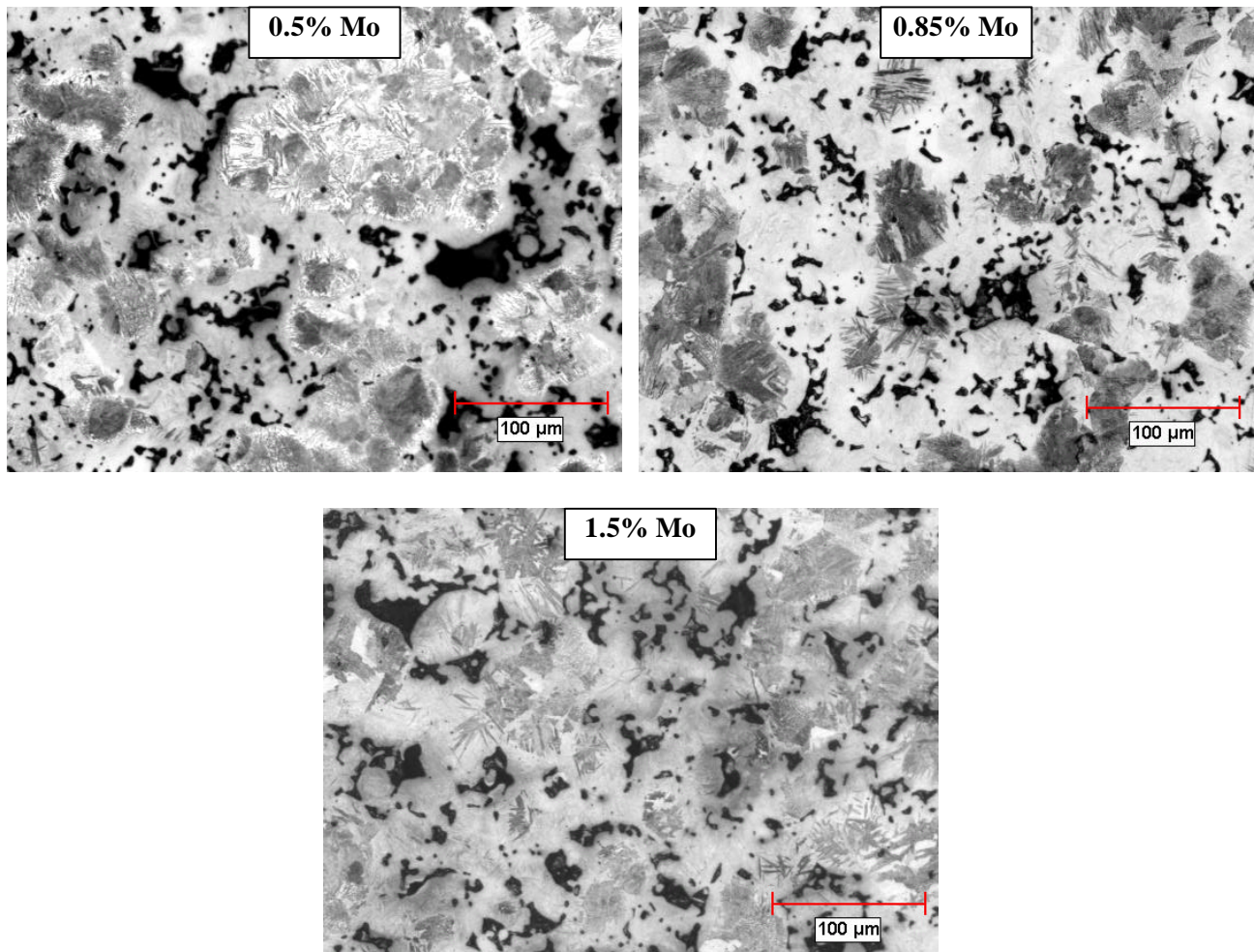


**Figure 6.** Typical microstructure of regular mixes made with 0.5, 0.85 and 1.5% Mo steel powders admixed with 4%Ni, 1.5%Cu and 0.6% graphite. (Specimens pressed to 7.0 g/cm<sup>3</sup>).

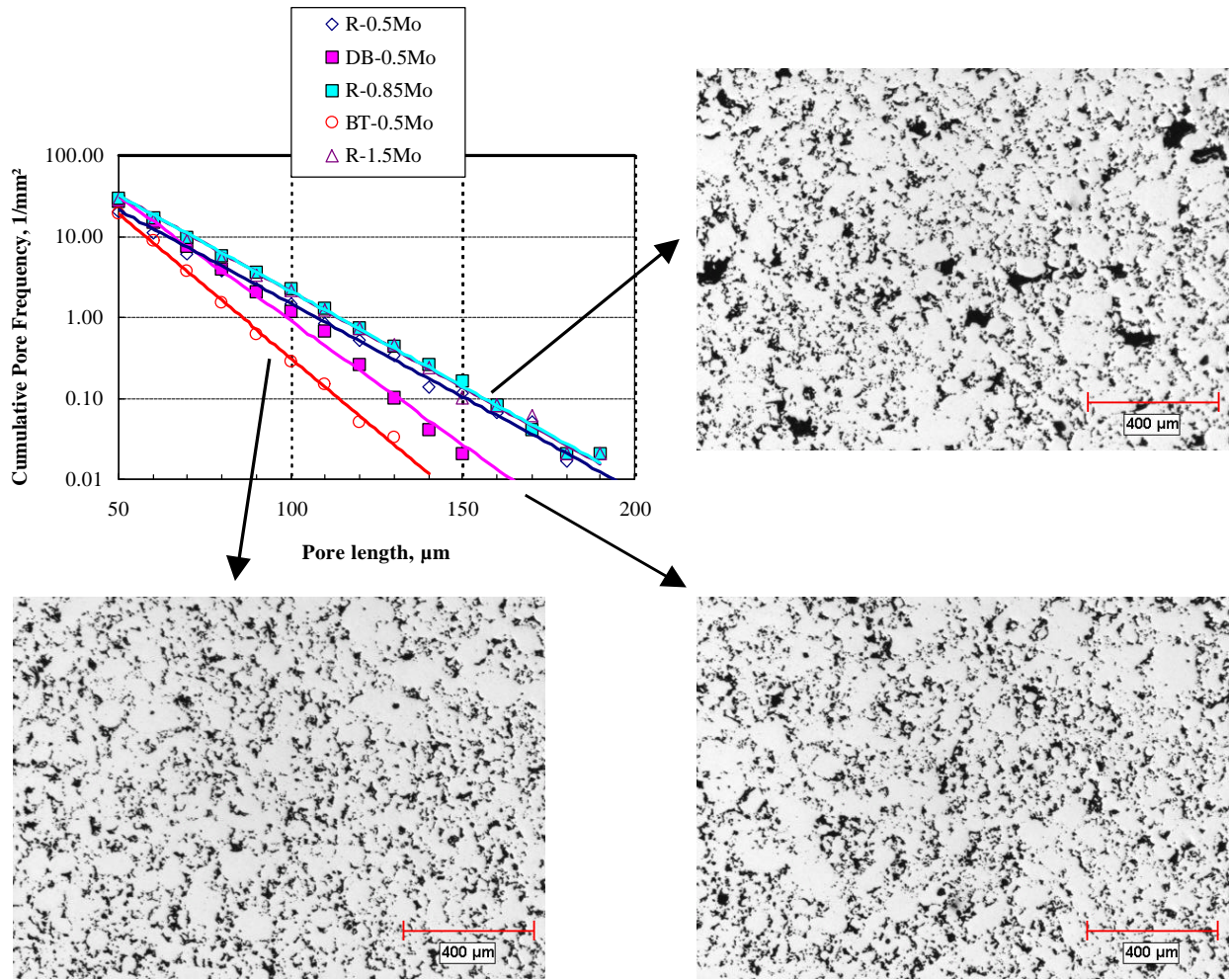


*Figure 7. Variation of the cumulative pore frequency (number of pores per unit area) for the regular, binder-treated and diffusion-bonded powders along with micrographs showing the porosity.*

## **Impact Energy**

The impact strength measured for all the materials evaluated in the study is shown in Figure 8. Typically, the impact energy ranged from 20.8 to 23.6 Joules. Raising the Mo content led to a slight decrease in impact strength, the difference being statistically significant. No significant difference in impact energy was found between the 0.5% Mo regular and the binder-treated materials, indicating that the size of Cu has no significant influence at 7.00 g/cm<sup>3</sup>. However, the use of a finer copper grade could have an effect on the impact energy at higher density. The impact energy of the diffusion-bonded material was slightly lower than that achieved with the two other materials for the 0.5% Mo series. It is worth mentioning that the impact energy was directly proportional to the elongation for all the materials. Finally, it is interesting to note that the variation in impact energy from one specimen to another increased with an increase in Mo content as indicated by the standard deviation shown in Figure 8 (Y error bar).

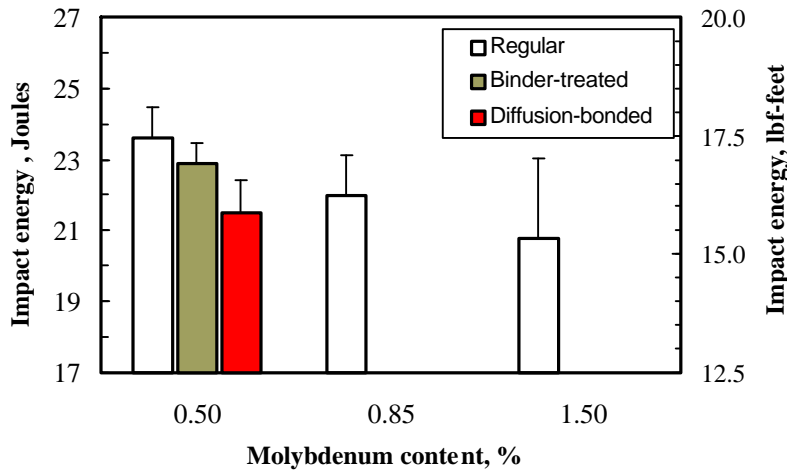


**Figure 8.** Impact energy obtained with powder mixes having different level of pre-alloyed Mo at 7.0 g/cm<sup>3</sup> (Mix formulation : 4%Ni, 1.5%Cu, 0.6% graphite).

## **Fatigue properties**

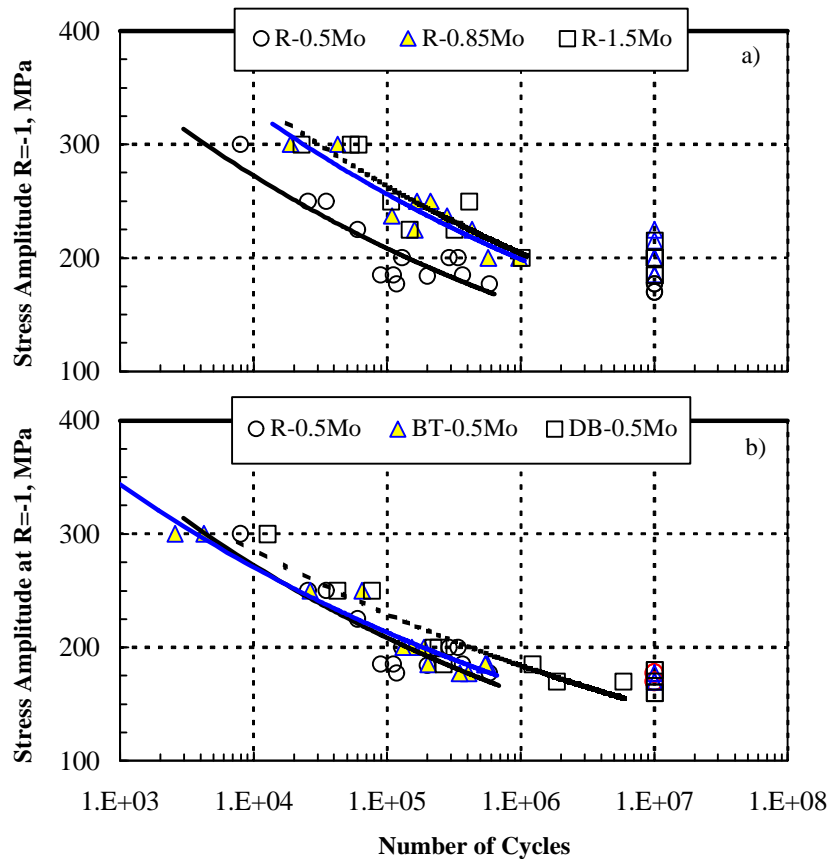
### **1. S-N curves (Influence of Mo content, types of mixes)**

Figure 9a shows the SN-curves obtained for the regular materials containing various level of pre-alloyed Mo while Figure 9b shows the S-N curves for the regular, binder-treated and diffusion-bonded materials containing about 0.5% pre-alloyed Mo. Equations of the type  $\log(S) = A + B \cdot \log(N)$  where S is the stress amplitude, N the number of cycles to reach failure and A and B coefficients was used in this work to characterize the S-N curves. It can be seen in Figure 9a that increasing the Mo content from 0.55 to 0.85% is clearly beneficial to the fatigue properties by shifting the S-N curves upward or to the right. However, no significant difference in the response to the cyclic loading was found between 0.85 and 1.5% Mo, both steel powders giving almost identical S-N curves.

No important difference in S-N curves was seen for the 0.5%Mo series, Fig. 9b. Both the regular and binder-treated mixes gave almost identical S-N curves while the S-N curve for the DB-0.5Mo material was slightly shifted upward or to the right. The average number of cycles for occurrence of failure for a given stress amplitude was lower for all of the 0.5% Mo series materials compared to the 0.85 and 1.5% Mo series. It is clear based on these results that the use of a finer copper, which resulted in a significantly lower quantity of pores larger than 50  $\mu\text{m}$ , has no significant effect on the S-N curve obtained on specimens pressed to 7.0 g/cm<sup>3</sup>. However, the use of fine copper could be beneficial at higher densities.

The variability of the fatigue-life can be expressed by the standard deviation or the standard error of the S-N curve equations [12]. These values were computed for each material and are given in Table III along with the parameters of the equations. The regular mix made with a 0.5%Mo steel powder (R-0.5Mo) showed the largest standard deviation amongst all the materials tested while the binder-treated material (BT-0.5Mo) showed the lowest standard deviation. A F-test showed that the difference in standard deviation between both materials was statistically significant at a confidence limit of 95%. It appears thus that the use of a finer copper combined with the binder-

treatment, which reduced significantly the number of large pores, reduced the variability in fatigue-life. The differences in variability between the binder-treated material and the other materials were not large enough to be statistically different at a 95% confidence level. However, the F-tests indicated that the probability that there exists a difference between the binder-treated material with fine copper and the other materials is 75% or higher. More tests would be needed to clearly confirm if there is a difference in variability is significant. In the same manner, the differences in standard deviation between the regular 0.5%Mo mix showing the largest variability and the other regular mixes with 0.85 and 1.5% Mo were not large enough to conclude with a level of confidence of 95% that these differences were significant. The probability that such differences are significant remains still elevated (between 77 and 83%).



**Figure 9.** S-N curves obtained at 7.0 g/cm<sup>3</sup> for Mo steel powder admixed with 4%Ni, 1.5% Cu and 0.6% graphite. a) Effect of molybdenum content b) Effect of powder manufacturing.

**Table III.** Parameters for the S-N curve equations.

Mix	Log(S) = A + B*log(N)				
	A	B	Std dev.	R value	R <sup>2</sup> value
R-0.5Mo	2.902	-0.1167	0.0372	0.8648	0.7479
R-0.85Mo	2.959	-0.1101	0.0290	0.9263	0.8581
R-1.5Mo	2.976	-0.1111	0.0297	0.8829	0.7795
R-0.5Mo	2.902	-0.1167	0.0372	0.8648	0.7479
BT-0.5Mo	2.847	-0.1037	0.0227	0.9657	0.9326
DB-0.5Mo	2.839	-0.0958	0.0325	0.9355	0.8752

## 2. Fatigue limit

The axial fatigue limit at 50% and 90% survivals as well as the tensile properties are reported in Table IV. Fatigue limits at 50 and 90% survivals are also shown in Figure 10. The fatigue limit where 50% of specimens should survived varied between 170 and 210 MPa, giving fatigue limit to tensile strength ratio of between 0.20 to 0.23. Increasing the Mo content from 0.5 to 0.85% was beneficial for the fatigue limit that increased from about 175 MPa to 210 MPa. Raising the Mo content up to 1.5% Mo did no yield to an additional gain in fatigue endurance which remains unchanged at 210 MPa. The better performance of the 0.85 and 1.5% Mo steel powder is likely due to the change in microstructure, mainly within steel particles from a more pearlitic type (fine and divorced) to a more bainitic/martensitic type [13].

**Table IV.** Tensile and axial fatigue limits of regular and diffusion-bonded Mo steel powders containing 4% Ni, 1.5% Cu and 0.6% graphite at 7.0 g/cm<sup>3</sup>.

Mix	UTS, MPa	YS, MPa	App. Hard. (test bars), HRC	Fatigue limit 50% survivals, MPa	Fatigue Limit 90% survivals, MPa	Endurance ratio FL <sub>50%</sub> /UTS
R-0.5Mo	854.0	544.7	19.0	177	162	0.21
BT-0.5Mo	834.4	566.5	19.7	176	161	0.21
DB-0.5Mo	847.7	543.6	22.3	168	160	0.20
R-0.85Mo	924.2	579.8	26.0	208	187	0.22
R-1.5Mo	936.8	587.2	26.0	211	183	0.23

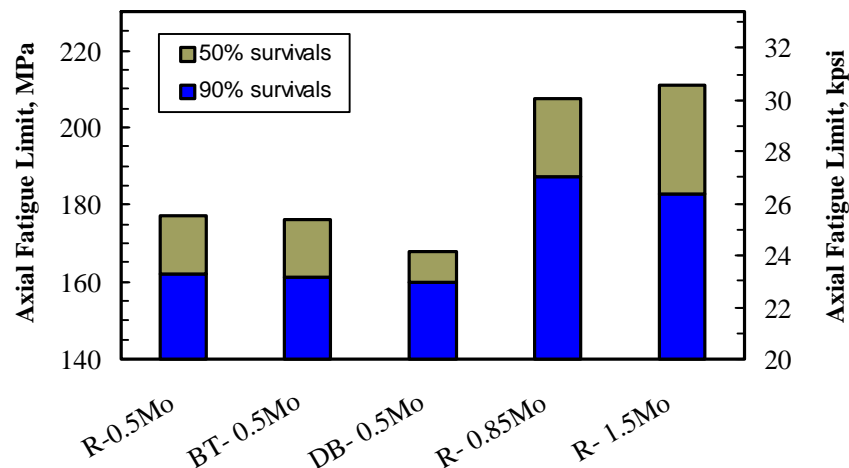


**Figure 10.** Fatigue limit at 50 and 90% survivals measured by the stair case method for different pre-alloyed Mo steel powder mixes at 7.0 g/cm<sup>3</sup>.

No significant difference in the fatigue limit was obtained between the specimens made with powder mixes containing 0.5% Mo. In all cases, the fatigue limit remained between 170 and 180 MPa. This result in combination with the S-N curves shown previously indicates that the use of finer copper did not have the anticipated beneficial effect on the fatigue limit for specimens pressed to 7.0 g/cm<sup>3</sup>. Indeed, as shown by different studies, pores play a key role in fatigue cracks initiation. In particular, the large pores are mainly contributing to fatigue crack initiation and propagation. It was clearly demonstrated in that study that the use of finer copper grade

reduced significantly the size of pores as well as the number of pores larger than 50  $\mu\text{m}$ . However, this had no significant effect on fatigue properties. A possible reason for that is, at 7.0  $\text{g/cm}^3$ , the volume fraction and thus, the quantity of large pores that could play a role in fatigue crack initiation, remains significantly high enough to contribute to fatigue. Also, in addition to porosity, the microstructure is another factor that strongly affects the fatigue properties. Indeed, at relatively low density, 7.0  $\text{g/cm}^3$  or lower, the strength of the sintering necks are believed to control fatigue [14]. However, it is clear from that study that modifying the microstructure within steel particles by increasing the Mo content had a significant influence on the fatigue endurance limit. It was indeed the key factor in that study.

Values reported in Table IV and Figure 10 are inferior to the fatigue limits obtained with the RBF test method and published in previous studies [3,7], see Fig. 2. The axial fatigue limit obtained for the 0.85% Mo powder is about 25% lower than the RBF limits shown in Figure 2. The mean axial fatigue limit at 50% survivals to tensile strength ratio (endurance ratio) achieved in that study was between 0.20 to 0.23 as compared to about 0.30 in previous studies. It is worth mentioning that no difference in tensile properties was obtained between these different tests. Therefore, the difference in endurance ratio is only due to a shift in the fatigue limit related to the test method.

It is known that the testing method selected to measure the response of a material to a cyclic loading has a strong influence on the results. Indeed, RBF tests usually yields to higher fatigue limit than the axial fatigue tests. Lin et al showed that the axial fatigue limit corresponded to about 78 to 92% the RBF limit for different as-sintered and heat-treated materials [15]. The major reason for such a difference is that during RBF tests, the stress is maximized only at the circumference of the specimens while during axial fatigue test, the stress is similar all across the tested surface area. In axial fatigue testing, the cracks could even initiate within the all tested surface area if defect significantly large are present even if fatigue cracks usually initiates at the surface or close to the surface for these types of specimens [16].

Selection of test specimen has also a significant effect. Indeed, in axial fatigue testing, circular specimens such as those used in RBF testing and flat bar specimens can be used. The former type of specimens is usually machined out of sintered blanks. The surface of these specimens consists in a thin layer of smeared material free of porosity [16]. In addition, there is no stress raiser factor along the circumference. Contrary to that, the surface of the flat bar specimens is in the as-sintered condition. Therefore, pores are open to the surface. Also, flat rectangular bars have corners that act as stress raiser sites. Fractographic analyses clearly showed that most of the fatigue cracks initiated from a corner and propagated to the opposite corner. This observation is in accordance with other studies that used identical fatigue specimen geometry [13]. Figure 11 shows different SEM micrographs of the fracture surface of a fatigue specimen made from mix R-0.5Mo. Fig. 11a shows a general overview of the fracture surface. The fatigue crack likely initiated from a large pore at the corner in region C, Fig. 11b. Fig. 11c shows region A closed to the initiation site. The fracture surface is typical of a fatigue crack-propagating mode with evidence of striations. Finally, region B shown in Fig 11d was a typical overload failure with evidence of ductile fracture. Typically, about 30 to 50% of the surface of specimens was in a fatigue crack-propagating mode while the balance was a typical ductile overload failure. The proportion of the surface area in the fatigue-propagating mode varied inversely to the stress amplitude. Therefore, presence of corners in flat specimens likely contributed to reduce the fatigue limit as compared to that would be obtained with machined circular specimens.

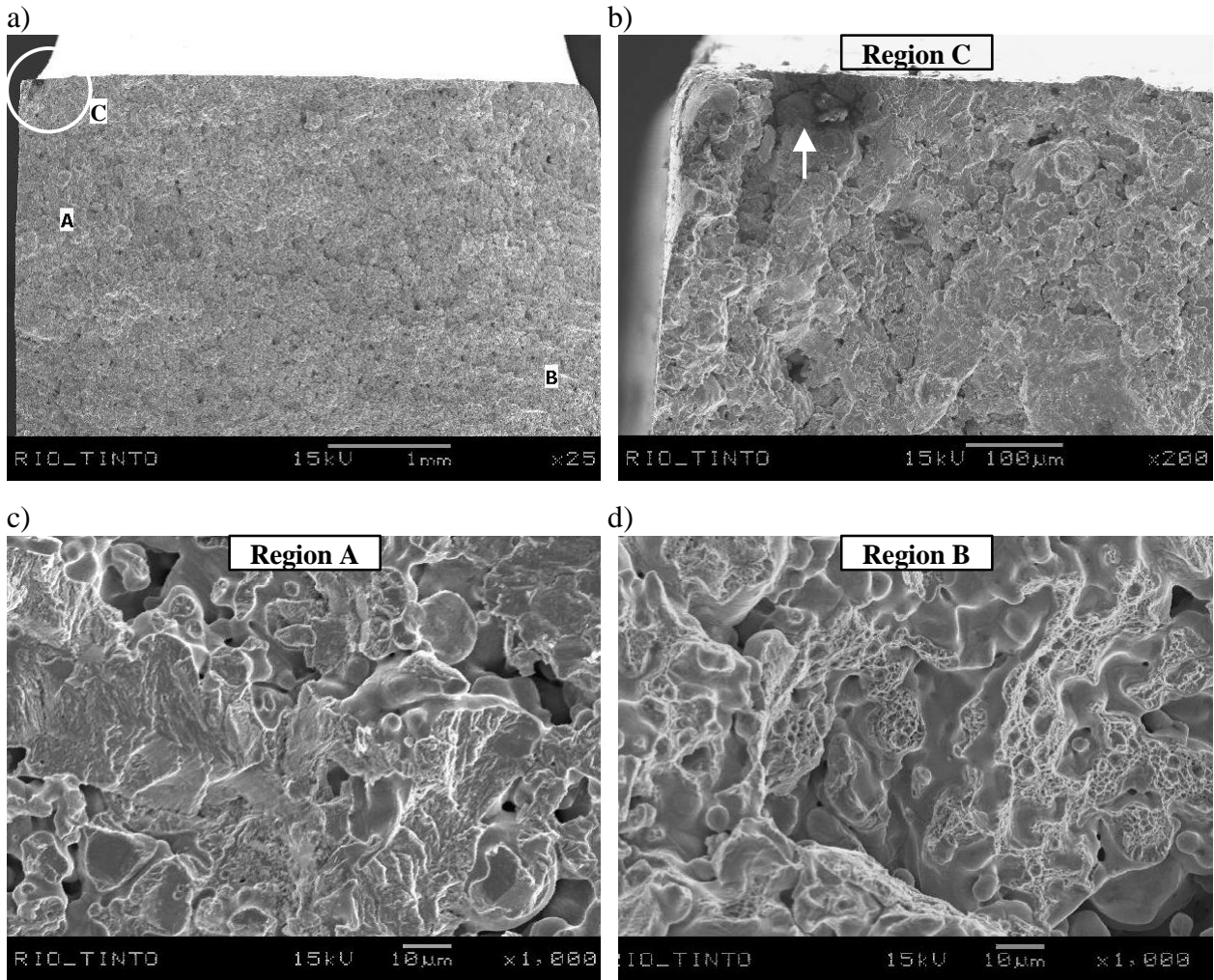


**Figure 11.** SEM Micrographs showing the fracture surface of a fatigue test sample (Mix R-0.5Mo).  
 a) Fracture surface at low magnification. b) Zone C : Fatigue crack likely initiated from a pore at the corner. c) Zone A: typical fatigue-propagating fracture mode. d) Zone B: Final ductile overload.

## CONCLUSIONS

A study on the influence of the amount of pre-alloyed Mo in low-alloyed steel powder on the static and dynamic properties of specimens containing 4%Ni, 1.5% Cu and 0.53% sintered carbon was carried out. The influence of using copper powders of different sizes was also investigated. Finally, the properties of regular and binder-treated mixes were compared to that of a diffusion-bonded material having the same composition. The following conclusions can be drawn:

- Increasing the Mo content from 0.5 to 0.85% was beneficial to the transverse rupture, tensile and fatigue properties but led to a slight decrease in elongation and impact energy.
- A further increase of the Mo content from 0.85 to 1.5% had no significant effect on the static and dynamic properties.
- The beneficial effect of increasing the Mo content from 0.5 to 0.85% on fatigue properties is explained by the transformation of the microstructure within steel particles from a divorced pearlite/pearlite type to a bainite/martensite type.

- Using fine copper resulted in a reduction of the size of pores and the number of pores larger than 50  $\mu\text{m}$  in length at a density of 7.0  $\text{g}/\text{cm}^3$ . This had no influence on the static properties except for the dimensional change which was more negative by about 0.08%.
- The reduction of the size of porosity caused by the use of finer copper led to less variation during cyclic loading. However, this had no influence on the S-N curve and fatigue limit at 7.0  $\text{g}/\text{cm}^3$ . It is believed that use of finer copper should be beneficial at higher densities.
- No significant difference in the fatigue properties was seen between a low-alloyed Mo steel powder admixed with Ni and Cu and a diffusion-bonded powder of the same composition.
- The axial fatigue limit obtained with flat specimens were about 25% lower than the fatigue limit achieved by RBF.

## **ACKNOWLEDGMENT**

The authors express their thanks to Mr. Luc Thibodeau for his contribution to the experimental portion of the work.

## **REFERENCES**

- 1 K.D. Christian, R.M. German and A.S. Paulson, Modern Development in P/M, Proc. Int. Conf., MPIF, Orlando, 1988, vol. 21, p. 23-39.
- 2 B. Lindqvist, Modern Development in P/M, Proc. Int. Conf., MPIF, Orlando, 1988, vol. 21, p. 67-82.
- 3 F. Chagnon and Y. Trudel, SAE paper, 1996, p.
- 4 P. Weiss and M. Dalgic, Advances in P/M and Particulate Materials, Proc. World Congress, Washington, MPIF, vol. 4, p (13) 249-257.
- 5 O. Mars, S. Bengtsson and A. Bergmark, Advances in P/M and Particulate Materials, Proc. Int. Conf., Vancouver, MPIF, 1999, vol. 2, p. (7) 157-161.
- 6 Y. Trudel and M. Gagné, Advances in Powder Metallurgy, MPIF, , 1989, Vol. 1, pp. 63.
- 7 Y. Trudel and F. Chagnon, Powder Metallurgy World Congress, Paris, EPMA, 1994, vol. 2, p. 815-818.
- 8 C. Gélinas and S. St-Laurent, Papier SAE, 2002, p.
- 9 F. Gosselin, "Segregation-Free Metallurgical Powder Blends Using Polyvenyl Pyrrolidone Binder", U.S. patent no. 5,069,714.
- 10 F. Chagnon and M. Gagné, Advances in P/M and Particulate Materials, Proc. Int. Conf., New York, MPIF, 2000, p. (13) 37-48.
- 11 G. Krauss, "Steels : Heat Treating and Processing Principles", American Society for Metals, Materials Parks, OH, 1990, p. 43-85.
- 12 R. C. Rice, "Fatigue Data Analysis", Metals Handbook ninth Edition, American Society for Metals, Metals Park, 1985, vol. 8, p. 695-712.
- 13 S. Bengtsson, Proc. Int. Conf., New York, MPIF, 2000, p. (6) 69-80.
- 14 A. Hadrboletz and B. Weiss, International Materials Reviews, 1997, vol. 42, no. 1, p. 1-44.
- 15 S.-Y. Lin, T. Prucher and T. Friedhoff, "Advances in Powder Metallurgy", Proc. Int. Conf., Toronto, MPIF, 1994, vol. 2, p. 381-389.
- 16 R.C. O'brien, Progress in Powder Metallurgy, Proc. Int. Conf., MPIF, 1987, vol 43, p.761-795.